


Temperature reduction in PPR pipes embedded in masonry

Redução de temperatura em tubos de PPR embutidos em alvenaria

Reducción de temperatura en tuberías de PPR empotradas en mampostería

Takashi Uehara* 

Instituto Federal de Educação, Ciência e
Tecnologia de São Paulo; *Campus* São Paulo;
Departamento de Construção Civil.
São Paulo (SP), Brasil

Armando Traini Ferreira 

Instituto Federal de Educação, Ciência e
Tecnologia de São Paulo; *Campus* São Paulo;
Departamento de Construção Civil.
São Paulo (SP), Brasil.
traini@ifsp.edu.br

* Corresponding author.

CRediT

Authors contribution: Conception, Data Curation, Methodology, Software, Supervision, Validation, Writing-Original Draft; Writing-Review & Editing: UEHARA, T.; Conception, Data Curation, Analysis, Data Collection, Methodology, Software, Supervision, Validation, Visualization, Writing-Original Draft; Writing-Review & Editing: FERREIRA, A. T.

Conflicts of interest: The authors certify that there is no conflict of interest.

Funding: Does not apply.

Ethical approval: The authors certify that there was no need for Ethics Committee approval.

A.I.: The authors certify that no artificial intelligence was used in the preparation of the work.

Editors: Daniel Sant'Ana (Editor-in-Chief); Ricardo Prado Abreu Reis (Guest Editor); Heber Martins de Paula (Guest Editor); Simone Buiarte Brandão (Editorial Assistant); Sarah Adorno Blanco Vencio (Editorial Assistant).

Abstract

During hot water transport through pipelines, heat is transferred to the surroundings, leading to a reduction in water temperature. It is the responsibility of building system designers to estimate thermal losses in hot water systems; however, the available data for different configurations and operating conditions are insufficient. This article aims to determine the temperature reduction in the flow of hot water in polypropylene random copolymer (PPR) pipes embedded in masonry, considering different pipe diameters and flow velocities. For this purpose, a model was developed with formulations based on heat transfer literature and Computational Fluid Dynamics simulations were conducted. The *t*-test indicated that the temperature reduction results obtained by the two methods were significantly different for the 20 mm pipe ($t = 2.7516$ and $p\text{-value} = 0.02961$) and 25 mm pipe ($t = 3.0391$ and $p\text{-value} = 0.02080$); however, the differences remained approximately constant when varying the velocity. Considering the characteristics of each approach, it can be concluded that the model shows promise and could serve as an option for estimating thermal losses in pipes, although further understanding of the phenomenon through experimental tests is necessary.

Keywords: Building hot water system; Temperature reduction; Thermal loss; PPR piping; Masonry; CFD.

Resumo

No transporte de água quente através de tubulações, ocorre transferência de calor para o ambiente, ocasionando a redução da temperatura da água. Cabe aos projetistas de sistemas prediais de água quente estimar as perdas térmicas, contudo, os dados disponíveis para diferentes configurações e condições de operação são insuficientes. Este artigo visa determinar a redução de temperatura no escoamento de água quente em tubulações de polipropileno copolímero random (PPR) embutidas em alvenaria, considerando diferentes diâmetros de tubo e velocidades de escoamento. Para isso, foi elaborado um modelo com formulações fundamentadas na literatura de transferência de calor, e foram realizadas simulações de Dinâmica dos Fluidos Computacional. O teste-*t* indicou que os resultados de redução obtidos pelos dois métodos foram significativamente diferentes para os tubos de 20 mm ($t = 2,7516$ e $p\text{-valor} = 0,02961$) e 25 mm ($t = 3,0391$ e $p\text{-valor} = 0,02080$), porém, as diferenças se mantiveram aproximadamente constantes ao variar a velocidade. Considerando as características de cada abordagem, conclui-se que o modelo é promissor e pode representar uma opção para a estimativa da perda térmica nos tubos, sendo necessário um aprofundamento da compreensão do fenômeno com a realização de ensaios.

Palavras-chave: Sistema predial de água quente; Redução de temperatura; Perda térmica; Tubulação de PPR; Alvenaria; CFD.

Resumen

En el transporte de agua caliente a través de tuberías, se produce una transferencia de calor al entorno, lo que resulta en una reducción de la temperatura del agua. Corresponde a los diseñadores de sistemas de agua caliente en edificios estimar las pérdidas térmicas, pero los datos disponibles para diferentes configuraciones y condiciones de operación son insuficientes. Este artículo tiene como objetivo determinar la reducción de temperatura en el flujo de agua caliente a través de tuberías de polipropileno copolímero random (PPR) empotradas en mampostería, considerando diferentes diámetros de tubería y velocidades de flujo. Para ello, se desarrolló un modelo basado en la literatura de transferencia de calor, y se realizaron simulaciones de Dinámica de Fluidos Computacional. La prueba *t* indicó que los resultados de reducción obtenidos por los dos métodos fueron significativamente diferentes para las tuberías de 20 mm ($t = 2.7516$ y $p\text{-valor} = 0.02961$) y 25 mm ($t = 3.0391$ y $p\text{-valor} = 0.02080$), sin embargo, las diferencias se mantuvieron aproximadamente constantes al variar la velocidad. Considerando las características de cada enfoque, se concluye que el modelo es prometedor y puede representar una opción para estimar la pérdida térmica en tuberías, siendo necesario profundizar la comprensión del fenómeno mediante la realización de ensayos.

Palabras-clave: Sistema de agua caliente en edificios; Reducción de temperatura; Pérdida térmica; Tubería de PPR; Mampostería, CFD.

1 Introduction

Access to hot water for sanitary use is considered a basic necessity (Borges, 2000). According to Chaguri Junior (2009), the volume of hot water consumed exclusively for bathing can account for approximately 6% to 12% of the total consumption in Brazil. Moreover, hot water systems in buildings are responsible for a significant amount of the country's energy consumption. These systems should be designed to operate efficiently, optimizing energy use and minimizing environmental impact.

In hot water flow through a pipeline, the temperature difference between the water and its surroundings results in heat transfer between these mediums, causing a reduction in the fluid's internal temperature (Incropera *et al.*, 2008). To avoid the need for increased energy consumption to obtain comfortable water temperatures, thermal losses should be minimized, which can be achieved with well-designed systems. Good energy performance of the hot water system can be obtained by using pipes made of appropriate materials, such as Polypropylene Random Copolymer (PPR), a plastic material with low thermal conductivity, classifying it as a thermal insulator (Tigre, 2012).

According to NBR 5626 (ABNT, 2020), thermal losses must be estimated by designers based on the materials used, as well as the system's configuration and operation. Estimating the temperature drop in the pipeline is crucial to understanding the amount of energy needed to compensate for this loss so as to select appropriate equipment and materials allowing for accurate predictions of energy costs.

Technical manuals provided by PPR pipe manufacturers generally include data on thermal energy loss in pipelines based on simplified formulas. These formulas often do not account for the different heat transfer modes in systems, nor do they consider variations in important parameters, such as flow rate and pipeline configuration. It should be mentioned that there is a lack of studies that determine more accurate calculation methods.

Chaguri Junior (2009) studied thermal losses in hot water pipelines, focusing on heat transfer through pipe walls. Another study, conducted by Ywashima, Ilha, and Ferreira (2017), considered both conduction through a pipe wall and internal and external convection, using convection heat transfer coefficients from the literature. Cardoso, Damo, and Matter (2007) experimentally compared the performance of different pipe materials and thermal insulations for hot water conduction in a masonry wall.

Uehara, Nascimento, and Ferreira (2022) presented a model to determine the temperature reduction in exposed PPR PN 25 pipes, taking into account all heat transfer modes, as well as various flow rates and pipe diameters. They compared the results with Computational Fluid Dynamics (CFD) simulations performed using Ansys®.

Uehara and Ferreira (2022a) conducted a study comparing a theoretical model for temperature reduction in pipes embedded in masonry with simulation results in Ansys®, using PPR PN 25 pipes with a DN20 diameter and varying the flow rates. Uehara and Ferreira (2022b) also carried out a similar study, but the variable parameter was the water flow velocity. However, these studies did not include an analysis to determine the appropriate value for the height of the wall section within the model's control volume, a critical parameter for convection and radiation analysis that influences the thermal loss in the pipe.

There are few studies on this topic addressing solutions that cover a limited range of boundary conditions. Therefore, this article aims to determine the temperature reduction in the hot water flow through PPR pipes embedded in masonry, considering different pipe diameters and flow velocities, and to determine the ideal height of the wall section in the theoretical model for the calculations.

2 Theoretical Foundation

Polypropylene Random Copolymer (PPR) is a polymeric raw material used to manufacture pipes and fittings, applicable in both hot and cold-water systems in buildings (Botelho and Ribeiro Junior, 2014). This material exhibits excellent thermal and mechanical properties, such as thermal stability and resistance to aging, making it suitable for piping systems in both domestic and industrial applications (Yu *et al.*, 2014).

A characteristic of PPR is its low thermal conductivity, classifying it as a thermal insulator (Tigre, 2012). This property allows for reduced heat loss from hot water to the surrounding environment. Moreover, concerning resistance to internal pressure, PPR pipes are categorized into three pressure classes: PN 25, PN 20, and PN 12.5. The latter is exclusive for cold water (Benedicto, 2009). PPR piping is specified by NBR 15813-1 (ABNT, 2018), which establishes nominal diameters (ND) ranging from 20 mm to 160 mm.

According to Borgnakke and Sonntag (2018), heat is defined as the transfer of energy across the boundary of a system at a given temperature to another system at a lower temperature. Considering a system in steady-state conditions, with fluid entering and exiting at different temperatures, the thermal energy equation can be expressed by Equation 1 (Borgnakke and Sonntag, 2018).

$$q = -\dot{m}c_p(T_{sai} - T_{ent}) \quad (1)$$

Where:

q = thermal energy outflow from the fluid (W);

\dot{m} = mass flow rate entering the system (kg s^{-1});

c_p = specific heat capacity at constant pressure of the fluid ($\text{J kg}^{-1} \text{K}^{-1}$);

T_{sai} = temperature of the fluid at the flow outlet (K);

T_{ent} = temperature of the fluid at the flow inlet (K).

According to Incropera *et al.* (2008), there are three heat transfer modes in a medium or between media: conduction, convection, and radiation. Conduction occurs through a stationary solid or fluid medium with a temperature gradient. Convection is the transfer of heat between a surface and a moving fluid, where both media have different temperatures. Radiation occurs between surfaces at different temperatures. Any surface with a non-zero temperature (above 0 K) emits energy in the form of electromagnetic waves. Thus, two surfaces at different temperatures exchange heat through radiation, provided there are no obstacles between them (Incropera *et al.*, 2008).

The amount of energy transferred per unit time can be obtained from appropriate rate equations for each transfer mode. For conduction, Fourier's law is used; for convection, Newton's law of cooling; and for radiation, Stefan-Boltzmann's law (Incropera *et al.*, 2008).

In the study of heat transfer, a one-dimensional system is one in which temperature gradients and, consequently, heat transfer occur in one direction (Incropera *et al.*, 2008).

According to Moran *et al.* (2005), cylindrical systems often exhibit temperature gradients in one direction, which is radial. Thus, these systems can be seen as one-dimensional.

In some situations, the consideration of one-dimensional conduction cannot be accepted due to the geometry of the medium. According to Incropera *et al.* (2008), multidimensional effects in these cases make two-dimensional conduction effects significant. Two-dimensional heat transfer problems can be solved using shape factors in the transfer rate equations, which are available in the literature addressing various geometries.

In problems involving heat transfer, it is common to consider a "circuit" of thermal resistances. Thermal resistance can be defined as the ratio between a temperature difference and the corresponding heat transfer rate, and it can be expressed by Equation 2 (Moran *et al.*, 2005).

$$R = \frac{\Delta T}{q} \quad (2)$$

Where:

R = thermal resistance ($K W^{-1}$);

ΔT = temperature difference (K);

q = heat transfer rate (W).

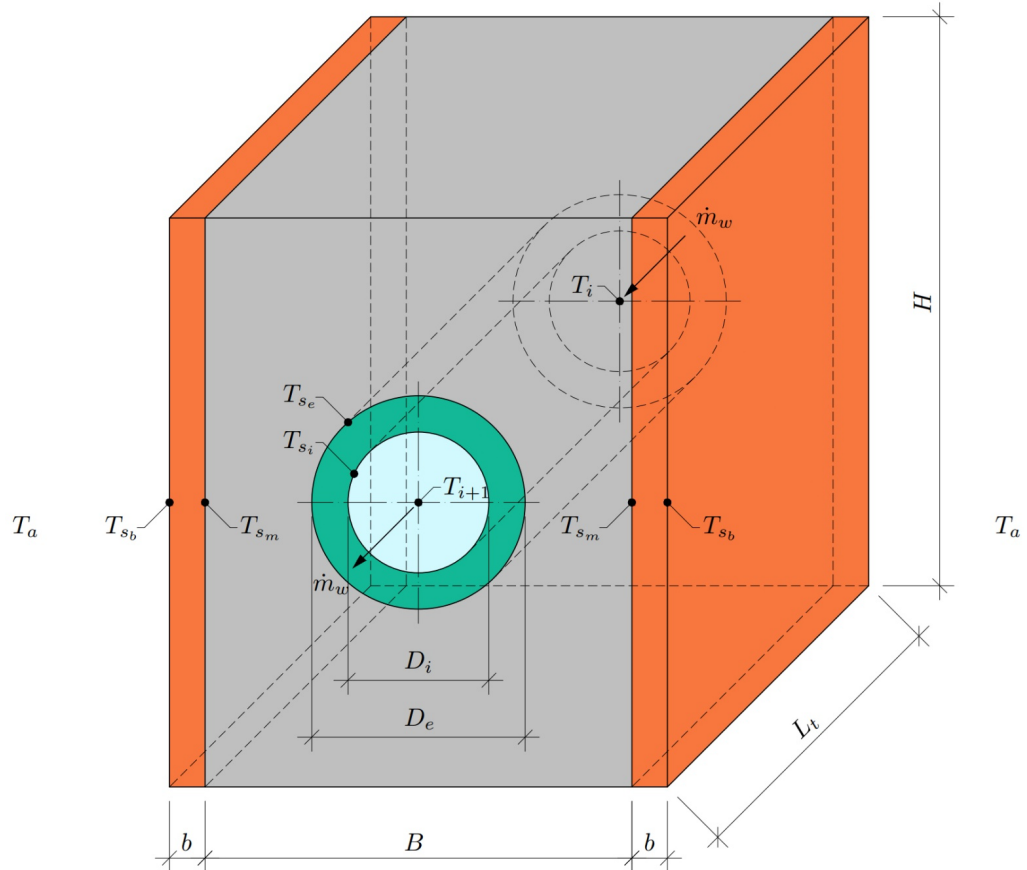
3 Methodology

A theoretical model was developed to calculate the temperature reduction in the flow through PPR pipes embedded in masonry, and computational simulations were conducted to compare the results of the two methods and evaluate the applicability of the model's formulations in estimating thermal losses in hot water piping systems in buildings. The theoretical model was then used to design a hot water system for a single-family residence to illustrate thermal loss determination in the pipes and the temperatures at points of use (sanitary fixtures).

3.1 Theoretical model

A steady-state system was considered in this study. This assumption means that the temperature reduction is calculated when the temperature at any point in the system remains constant, disregarding the period during which part of the thermal energy from the water is used to heat the pipes and the surrounding wall, which initially are at ambient temperature. The theoretical model (Figure 1) consists of a control volume that contains a "slice" of masonry wall, with a PPR pipe positioned at its center and air on the outer side. The masonry comprises a ceramic block represented by two plates (the orange solids in the figure) and mortar (gray solid) that surrounds the pipe.

Figure 1: Theoretical model.



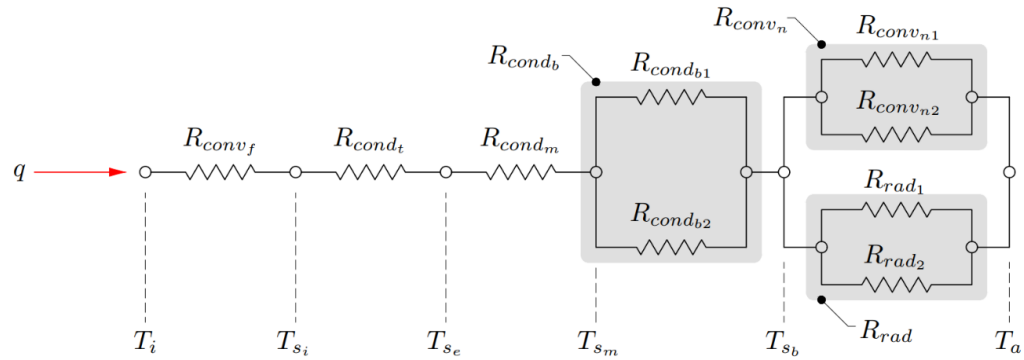
Legend:

- B = mortar width (m)
- b = block plates' width (m)
- D_e = pipe external diameter (m)
- D_i = pipe internal diameter (m)
- H = wall section height (m)
- L_t = pipe length (m)
- \dot{m}_w = mass flow rate of water (kg s^{-1})
- T_a = ambient temperature ($^{\circ}\text{C}$)
- T_i = upstream water temperature ($^{\circ}\text{C}$)
- T_{i+1} = downstream water temperature ($^{\circ}\text{C}$)
- T_{sb} = wall surface temperature ($^{\circ}\text{C}$)
- T_{se} = pipe external surface temperature ($^{\circ}\text{C}$)
- T_{si} = pipe internal surface temperature ($^{\circ}\text{C}$)
- T_{sm} = temperature of the mortar surface in contact with the block ($^{\circ}\text{C}$)

It was assumed that the faces on both sides of the wall (designated as side 1 and side 2) have the same temperature, and that the external air and the surrounding environment are at ambient temperature (T_a). The pipe carries water with a mass flow rate of \dot{m}_w . Upstream (inlet) of this section of the pipe (identified as section “i”, the water temperature is T_i , and downstream (outlet), the temperature is T_{i+1}). The objective of the model is to determine the downstream temperature based on the upstream temperature of a section, which corresponds to the upstream temperature of the subsequent section. Thus, the thermal loss from various sections i of a pipeline can be calculated.

To achieve a better approximation between the model and a real system, all heat transfer modes were considered, and the necessary empirical correlations were selected so that the system could meet the application conditions. The system can be represented using the thermal circuit, shown in Figure 2, utilizing thermal resistances for each heat transfer mode and each geometry element.

Figure 2: Thermal circuit of the theoretical model.



It was assumed that forced convection (R_{conv_f}) occurs between the water and the inner surface of the pipe, one-dimensional conduction in the radial direction within the pipe (R_{cond_t}), two-dimensional conduction in the mortar (R_{cond_m}), one-dimensional conduction in the block (R_{cond_b}) and natural convection and radiation acting in parallel between the wall surface and the surrounding environment (R_{conv_n} and R_{rad}). For the last three, heat flow occurs in parallel between sides 1 and 2 of the wall, as shown in Figure 2. Thus, the equivalent resistance for each mode was calculated. Moreover, the equivalent resistance of natural convection and radiation was calculated for each side.

The hot water flow in the system is turbulent. The Reynolds number was calculated using the formulation for internal flows in circular pipes, as presented by Brunetti (2008). To calculate the forced convection properties, it was assumed that the flow was fully developed (both hydrodynamically and thermally), meaning that the formulations are applicable in a part of the pipe that is sufficiently far from the inlet.

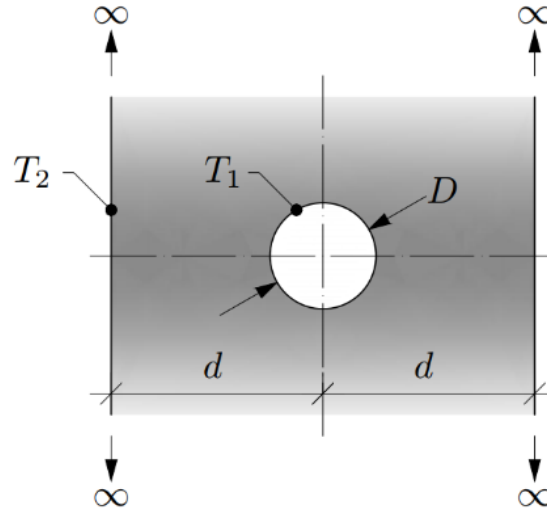
The Nusselt number was calculated using the Chilton-Colburn analogy, a widely accepted correlation for fully developed turbulent flow in smooth circular pipes (Incropera *et al.*, 2008). For the friction factor, the Swamee expression was used, which can determine the value of this property without any restrictions regarding the flow regime (Porto, 2006). The characteristic length of the surface for calculating the forced convection heat transfer coefficient corresponds to the internal diameter of the pipe.

For conduction in the pipe, the expression for calculating the conductive thermal resistance of a hollow cylindrical system was used, as obtained from Incropera *et al.* (2008) and Moran *et al.* (2005), which considers one-dimensional conduction in the radial direction. The ceramic block consists of two ceramic plates, one on each side of the masonry and in contact with the mortar. The thermal resistance of each plate was calculated using the expression for the conductive thermal resistance of a flat plate obtained from Moran *et al.* (2005).

In the mortar, two-dimensional conduction occurs, where energy is transferred from the external surface of the pipe to the mortar surfaces in contact with the block. Typically, a pipeline is embedded close to one side of the wall, resulting in an asymmetrical cross-

section of the system. To facilitate using a shape factor for conduction in the mortar, as found in the literature, the geometry was simplified to a centrally positioned pipe within the wall section, which is then compared to the actual asymmetrical geometry modeled in the computational simulations. An appropriate shape factor for this geometry was taken from Incropera *et al.* (2008), which addresses the scenario of a long horizontal circular cylinder positioned midway between two parallel, thick planes of equal length and infinite width, as expressed in Equation 3. The geometry for applying the shape factor is illustrated in Figure 3.

Figure 3: Geometry to determine the shape factor.



Source: Adapted from Incropera *et al.* (2008).

$$S = \frac{2\pi L_t}{\ln\left(\frac{4B}{\pi D_e}\right)} \quad (3)$$

Where:

S = shape factor (m);

L_t = pipe length (m);

B = mortar width (m);

D_e = pipe external diameter (m).

On both sides of the wall, heat transfer occurs through natural convection from the block to the air. The wall's geometry determined the formulation for natural convection for vertical plates. Consequently, the calculation of the Rayleigh number and the heat transfer coefficient for natural convection used the height of the wall as the characteristic length of the surface. The Nusselt number was determined using the Churchill and Chu correlation, a well-established expression for vertical plates in natural convection (Moran *et al.*, 2005).

For the radiation modeling, it was considered that the wall is surrounded on both sides by a surrounding surface at ambient temperature to utilize the equation presented by Incropera *et al.* (2008), which analyzes a surface exchanging energy with an isothermal surface (the surroundings) that envelops it. The air properties were evaluated at the film temperature, calculated as the mean between the surface temperature of the wall and the ambient temperature.

Temperature T_{sb} of the external wall surfaces is initially unknown; however, it is needed in order to calculate the convective and radiative thermal resistances. Its value was calculated using Equation 4, developed based on the rate equations of each transfer mode and considering the energy conservation in a steady-state system (the first law of thermodynamics), according to Borgnakke and Sonntag (2018). This affirms that the heat transfer rates in each mode have the same value (q).

$$T_{sb} = T_i - q (R_{convf} + R_{condt} + R_{condm} + R_{condb}) \quad (4)$$

Where:

T_{sb} = wall surface temperature (°C);

T_i = upstream water temperature of the pipe (°C);

q = heat transfer rate (W);

R_{convf} = thermal resistance of forced convection ($K W^{-1}$);

R_{condt} = conductive thermal resistance of the pipe ($K W^{-1}$);

R_{condm} = conductive thermal resistance of the mortar ($K W^{-1}$);

R_{condb} = conductive thermal resistance of the block ($K W^{-1}$).

To determine the correct value of T_{sb} , an iterative process was carried out, starting by assigning an initial value for this temperature. Using this value, all thermal resistances were calculated to determine the heat transfer rate using Equation 2. Next, the same temperature value was verified with Equation 4. If the stipulated and verified values were different, a new value was assigned, and the calculations were repeated. When the values matched, energy conservation was satisfied, and the downstream water temperature of the pipe was determined using the correct thermal resistance values.

T_{sai} was replaced by T_{i+1} and T_{ent} by T_i in Equation 1. The thermal energy output corresponds to the heat transfer rate from Equation 2. Thus, the expression used to determine the downstream water temperature of the pipe was obtained, as presented in Equation 5.

$$T_{i+1} = T_i - \frac{T_i - T_a}{\dot{m}_w c_p (R_{convf} + R_{condt} + R_{condm} + R_{condb} + R_{convn,rad})} \quad (5)$$

Where:

T_{i+1} = downstream water temperature of the pipe (°C);

T_i = upstream water temperature of the pipe (°C);

T_a = air and surrounding environment temperature (°C);

\dot{m}_w = mass flow rate of water ($kg s^{-1}$);

c_p = specific heat at constant water pressure ($J kg^{-1} K^{-1}$);

R_{convf} = thermal resistance of forced convection ($K W^{-1}$);

R_{condt} = thermal resistance of conduction in the pipe ($K W^{-1}$);

R_{condm} = thermal resistance of conduction in the mortar ($K W^{-1}$);

R_{condb} = thermal resistance of conduction in the block ($K W^{-1}$);

$R_{convn,rad}$ = equivalent thermal resistance of natural convection and radiation ($K W^{-1}$).

The theoretical model formulations were inserted into a spreadsheet using Microsoft® Excel®. To obtain the water and air thermophysical properties, the mini-REFPROP software (version 10.0) from the National Institute of Standards and Technology (NIST) was used. This tool can retrieve properties for various pure and pseudo-pure fluids (NIST, 2020).

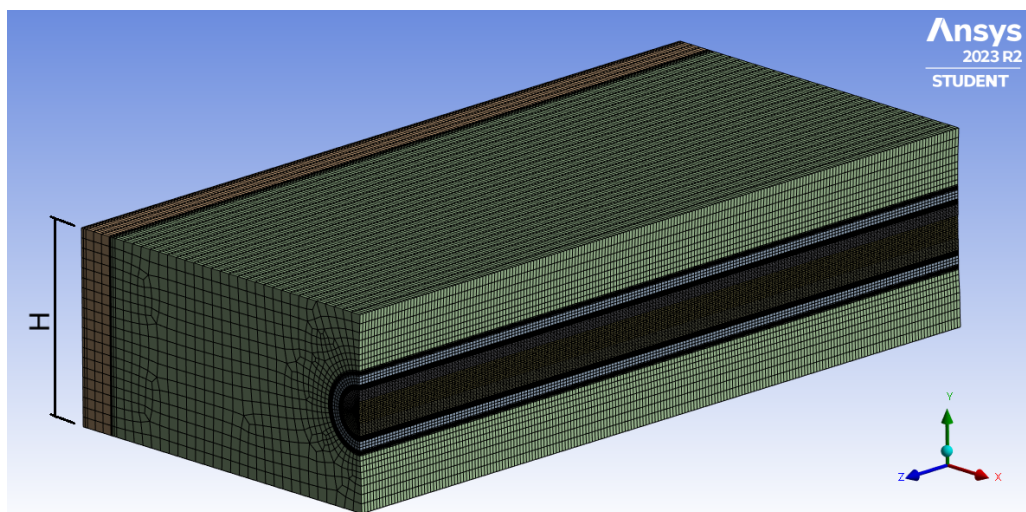
3.2 Computer simulator

For the simulations, the Ansys® Fluent 2023 R2 Student software (the academic and free version of Ansys® 2023 R2) was used. This software is based on Computational Fluid Dynamics (CFD) and is widely accepted and used in fluid mechanics and heat transfer analyses (Versteeg and Malalasekera, 2007). The equations used for solving the CFD simulations include mass, momentum, and energy conservation. Other important processes can be described by equations that are solved together with the conservation equations, such as turbulence, for which empirical models are used to reduce the computational power required for the simulations (Silva, 2019).

To apply the governing equations, a mesh of elements needs to be generated over the domain. In Fluent, the numerical solution method is the Finite Volume Method (FVM), in which the domain is divided into control volumes to integrate the equations in each element (Versteeg and Malalasekera, 2007). The proximity between the simulation solution and the exact solution depends on various factors, such as the size and shape of the control volumes (mesh quality) and the size of the errors (residuals) generated during iterations (Silva, 2019). As it is a free version, this program has a limitation of 1,048,576 elements in the mesh (Ansys Inc, 2023b).

Due to the fact that the geometry of the problem is quite simple (it has no curvatures in the flow or complex shapes), a structured mesh of hexahedral volumes was generated, as recommended by Ansys Inc (2023a). The mesh was created in the Ansys Meshing program, which is already incorporated into the package. The quality of the mesh was evaluated by the program itself, using aspect ratio, orthogonality, and skewness indicators. The latter two presented values that were considered good. The mesh was refined in the water flow domain to reduce the dimensions of the elements close to the inner surface of the pipe in the radial direction, aiming to simulate the conditions of the boundary layer more accurately. This resulted in the elements being elongated in the circumferential and longitudinal directions, leading to an acceptable aspect ratio. Figure 4 shows a section of the geometry with the mesh used in one of the simulations.

Figure 4: Mesh generated in Ansys Meshing.



The program was configured to perform the simulation based on pressure, which is one of the available methods for solving the conservation equations, typically used for

incompressible flows (Ansys Inc, 2023a). The standard $k - \varepsilon$ turbulence model was used, as the flow is simple (it has no curvatures, free flows, separated flows, among others), not requiring the advantages of more advanced models.

In the materials, the fluid properties (water and air) and solids (PPR, mortar, and ceramics) were defined. Fluent can specify the density, specific heat at constant pressure, thermal conductivity, and dynamic viscosity of the materials. The fluid properties were obtained from mini-REFPROP, the PPR properties were sourced from Amanco (2010) and Tigre (2012), and the mortar and ceramics properties were obtained from Incropera *et al.* (2008).

In the boundary conditions, the water temperature and velocity at the flow inlet were defined, as well as the thermal conditions at the boundaries. At all external boundaries (except the lateral ones), a thermal condition of zero heat flow was assigned to simulate the condition of an adiabatic wall. On the sides, a “mixed” condition for radiation and convection was imposed, where the convection heat transfer coefficient (which must be estimated, in this case, by the theoretical model), the free flow temperature (ambient temperature), and a value for surface emissivity were specified. The reported heat transfer coefficient is the natural convection coefficient calculated by the theoretical model, and the emissivity is that of the ceramic surface.

We decided to perform 250 iterations for each simulation. The residue values of the simulation decreased as the solution progressed and were stored and displayed in a graph. By default, Fluent's convergence criterion is 10^{-3} for all equations except for energy, which has a criterion value of 10^{-6} . All simulations in this research reached values below these criteria, indicating that the iterations were sufficient for the solution to converge to the final result.

The specified upstream velocity and temperature of the pipe are considered constant throughout the cross-section of the flow, which would only occur if the upstream face were the inlet of a pipeline. Thus, the simulation does not meet the theoretical model's assumptions regarding the developed flow condition. To correct this issue, a velocity profile downstream from the first simulation was exported and then imported into the program to be used as the upstream profile in the following simulation. Thus, the new simulation considered a developed flow at the inlet, fulfilling the premise of fluid dynamically developed flow throughout the entire length of the pipeline.

However, this process was not carried out for temperature, as the mean downstream temperature has a lower value than the temperature to be assigned upstream (40°C). Moreover, a developed downstream profile cannot be obtained with a mean temperature of 40°C, as this implies a null thermal flow, which only occurs if there is no temperature gradient in the profile.

3.3 Comparing the methods

When comparing the theoretical model and the simulations, the same boundary conditions were considered (dimensions of the masonry and the piping, inlet water temperature, ambient temperature, among others). The tested situation was a PN 25 PPR pipe embedded in solid ceramic brick masonry without coating. The analyses were conducted for nominal diameters DN20, DN25, and DN32 (commonly used in single-family homes) and different water flow velocities, aiming to verify the applicability of the formulation across a wide range of situations. The upstream water temperature was

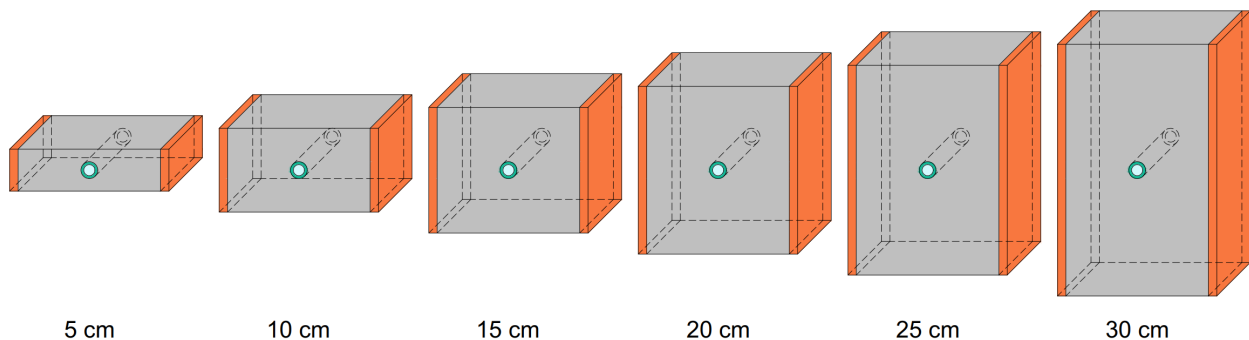
considered to be 40°C, the ambient temperature was 20°C, the pipe length was 20 cm, the internal wall width was 17 cm, and the external width was 19 cm.

To apply the theoretical model, a wall height (H) must be considered to calculate the thermal resistances of conduction in the block, natural convection, and radiation. The size of the wall to be considered influences the result of the temperature reduction calculation and must be appropriately chosen. The comparison was divided into two stages: in the first stage, a study was conducted to determine the wall height to be adopted for each diameter; in the second stage, the model was evaluated by comparing the methods, taking into account the height defined in the first stage while varying the water flow velocities.

3.3.1. First stage

In the first stage of the analysis, a comparison was made between the temperature reductions in the theoretical model and the simulations for walls heights of 5, 10, 15, 20, 25, and 30 cm (represented in Figure 5) and for velocities of 0.5 and 3.0 m/s. The geometry of the masonry adopted for these simulations is identical to that of the theoretical model to facilitate the variation of dimensions in the Fluent modeling, as determining the wall height does not require precision in the simulation results, and the mortar and ceramic have thermophysical properties with similar values, according to Incropera *et al.* (2008).

Figure 5: Wall Heights considered for the first stage.



To help choose the ideal height for the theoretical model application, the simulation results and the model were compared with two other models: one for the situation of an exposed pipe (not embedded in masonry) and an alternative model for an embedded pipe. The model for the exposed pipe is presented by Uehara, Nascimento, and Ferreira (2022), which considers heat transfer through the three modes (conduction, convection, and radiation) and uses a specific correlation for natural convection in horizontal cylinders.

The alternative model is similar to the theoretical model of this study, with only one change in the representation of the mortar. The geometry of the mortar was simplified to two vertical flat plates, both positioned between the pipe and the ceramic block plates. Thus, one-dimensional conduction occurs through each plate, eliminating the need for the form factor for two-dimensional conduction. The plates act in parallel, similar to the plates that comprise the block.

The value of the thermal resistances of the vertical plates representing the mortar in the alternative model depends on the wall height, unlike the theoretical model, where the resistance is calculated based on the form factor, which does not vary with height. In the alternative model, conduction in the mortar occurs unidimensionally, while in the theoretical model, conduction is bidimensional. It is considered that heat transfer in both

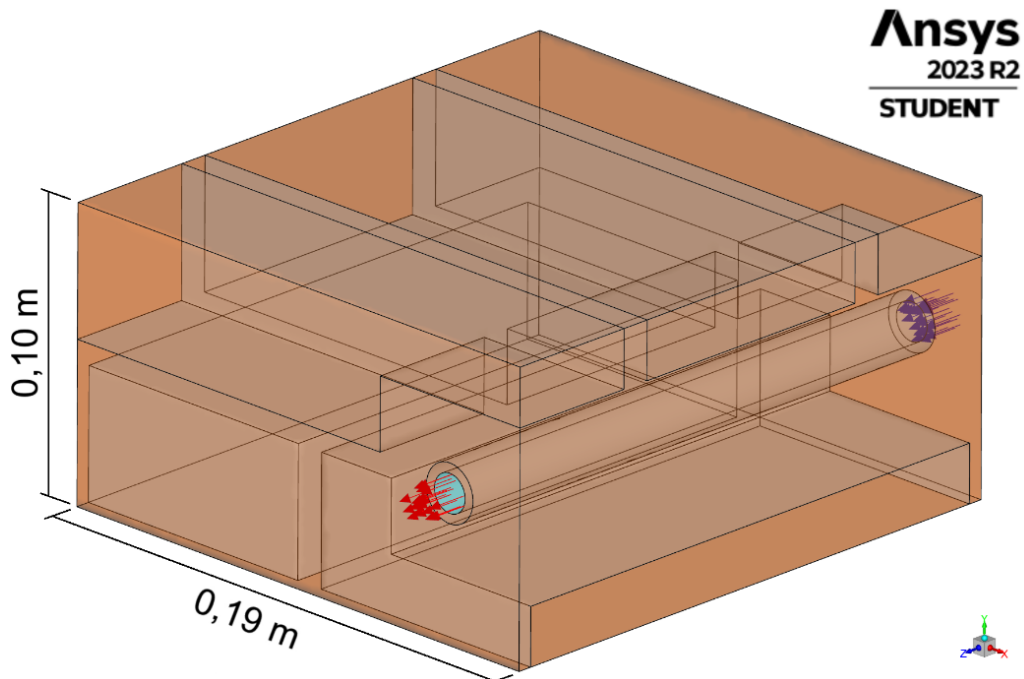
modeling approaches is similar, whereby heat is transferred from the hotter region (the surface of the pipe, which is at temperature T_{s_e} to the cooler region (the surface of the mortar in contact with the block).

Graphs were made using the temperature downstream results for each method (theoretical model, simulation, alternative model, and apparent pipe model) as a function of the wall height. This was done separately for each diameter and flow velocity. In each graph, the height at which the curves for the theoretical model and the simulation intersected were obtained, which corresponds to the height at which the methods result in the same temperature reduction. The wall height for each diameter was defined by averaging the heights found for the two velocities, rounded up to multiples of 0.05 m, according to the increment used for the tested heights. To evaluate the results, the proximity between the temperature reductions of the theoretical and alternative models at the intersection height was assessed. Close values of reduction also indicate that the conductive thermal resistances of the mortar in both models are similar.

3.3.2. Second stage

In the second stage, a new comparison was made between the two methods for each diameter, where the modeling in Fluent consisted of a pipe embedded in a wall with the usual geometry and pipe arrangement (solid ceramic bricks of 90x53x190 mm, uncoated, laid with 10 mm mortar, and the pipe embedded near one of the wall faces), as shown in Figure 6. In these simulations, flow velocities of 0.5, 1.0, 1.5, 2.0, 2.5, and 3.0 m/s were considered, as well as the wall height defined in the first stage.

Figure 6: Geometry for the simulations of the second stage for the DN20 pipe.



To evaluate the difference between the temperature reduction results from the theoretical model and the simulation, a statistical analysis was conducted for each diameter to test the difference between the means of the reductions from the two methods. Each reduction was calculated as the difference between the inlet temperature (40°C) and the outlet temperature. To apply the *t*-test, the normality of the samples was verified using the Shapiro-Wilk test with a significance level of 5%, according to Frei (2018).

The two reduction samples are dependent, as each element of one sample (theoretical model) corresponds to an element in the other sample (simulation) (Larson, 2023). Therefore, a *t*-test was performed for the difference between the means of two samples with paired data. The null hypothesis is $\mu_d = 0$, which means that the mean of the differences between the data is equal to zero, indicating that the results are significantly close. Thus, the alternative hypothesis is $\mu_d \neq 0$, indicating that there is a significant difference between the compared temperature reductions.

For the three diameters, a two-tailed test was chosen with a confidence level of 95% and 5 degrees of freedom. To accept or reject the null hypothesis, the test statistic and p-value were determined. The Shapiro-Wilk test and the calculation of the p-value for the *t*-test were performed using the statistical analysis software Jamovi (version 2.3.28.0) (Şahin and Aybek, 2019). Afterward, the percentage difference between the reductions was analyzed to check if this value remained constant as the water flow velocity varied.

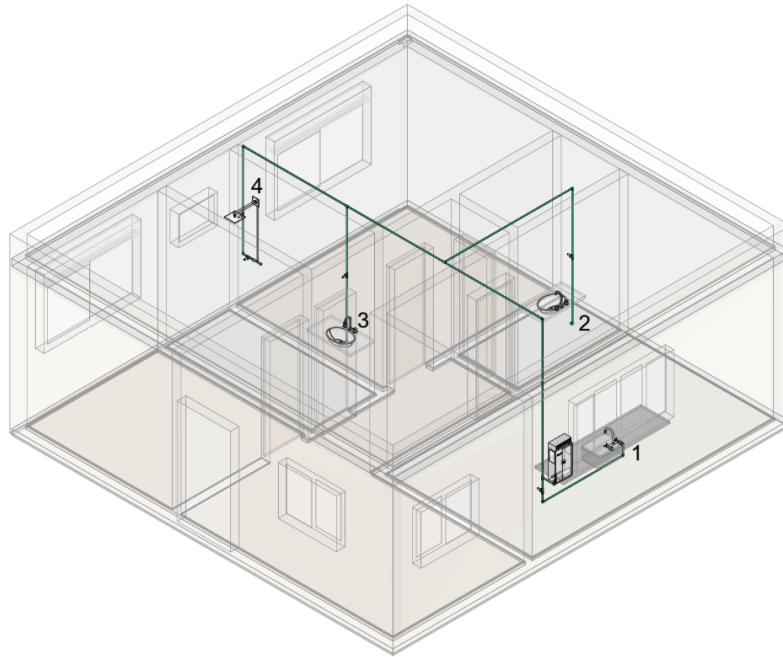
3.4 Temperature Loss in a Residential Hot Water System

To exemplify the theoretical model application, a project was developed for a residence consisting of a single-story house with two bedrooms, a living room, kitchen, laundry area, bathroom, and a lavatory. The structural system is made of reinforced concrete, and the walls consist of ceramic blocks 14 cm wide, coated with a 2 cm thick plaster. The roof consists of an exposed slab with parapets 40 cm high around the perimeter.

The hot water plumbing system in the residence is designed to serve the sanitary appliances in the kitchen (sink), lavatory (basin), and bathroom (basin and shower). Heating is done by a gas instantaneous heater installed in the outdoor area, which raises the water temperature from 20°C to 40°C. The hot water pipes are made of PPR PN 25 with a nominal diameter of DN20, embedded in the walls at a distance of 2 cm from the wall surface. In the slab, the pipes are embedded at a distance of 2 cm from the upper surface.

The isometric view in Figure 7 shows the residence and the hot water plumbing system. Numbers 1, 2, 3, and 4 indicate, respectively, the sink, the lavatory basin, the bathroom basin, and the shower. To minimize the accumulation of air or vapor in the pipes, as recommended by NBR 5626 (ABNT, 2020), an air vent valve can be installed in the section running through the ceiling, ensuring the proper functioning of the system

Figure 7: Isometric view of the residence.



For the theoretical model application, the non-simultaneous situation of the system was considered, meaning that only one appliance is used at a time, and the calculation was performed for the trajectory between the heater and the point of use for each of the appliances. All calculations considered a wall with an internal width of 0.14 m and a height of 0.10 m, and a block with a thickness of 0.02 m. For the sake of simplification, this configuration was also adopted for the pipes embedded in the slab. The hot water flow rates were determined using the weighted average method indicated in NBR 5626 (ABNT, 1998). The flow rate for the sink is 7.5 L/min, for the basins it is 4.5 L/min, and for the shower it is 6.0 L/min. Additionally, the ambient temperature was adopted at 20°C.

The temperatures at the points of use for each appliance were determined, as well as the temperature reductions relative to the temperature at the heater outlet, the energy losses in the pipeline, the energy used for heating, and the percentage of energy loss. The energy loss corresponds to the thermal energy output given by Equation 1. Heating energy corresponds to the amount needed to raise the water temperature from 20°C to 40°C, which was calculated without considering the efficiency of the heater.

4 Results and Discussion

4.1 First stage

Figure 8 presents the results for the downstream temperature as a function of wall height for each method for the DN20 pipe at a velocity of 0.5 m/s. It can be observed that the temperature reduction is greater in higher walls. This occurs because the increase in height reduces the conductive thermal resistances of the block and the equivalent natural convection and radiation resistances, which increases the heat transfer rate and, consequently, the temperature loss. In the alternative model, the reduction is even greater due to the dependence of the wall height on the formulation of the conductive thermal resistance of the mortar. It should be mentioned that this does not occur in the theoretical model, which uses a shape factor that is independent of the height. In the apparent pipe model, the thermal resistance of the system does not change due to the absence of a wall,

resulting in a higher value than that of the other models starting at a height of 10 cm, leading to lower thermal loss.

Figure 8: Downstream temperature for the DN20 pipe at a velocity of 0.5 m s⁻¹.

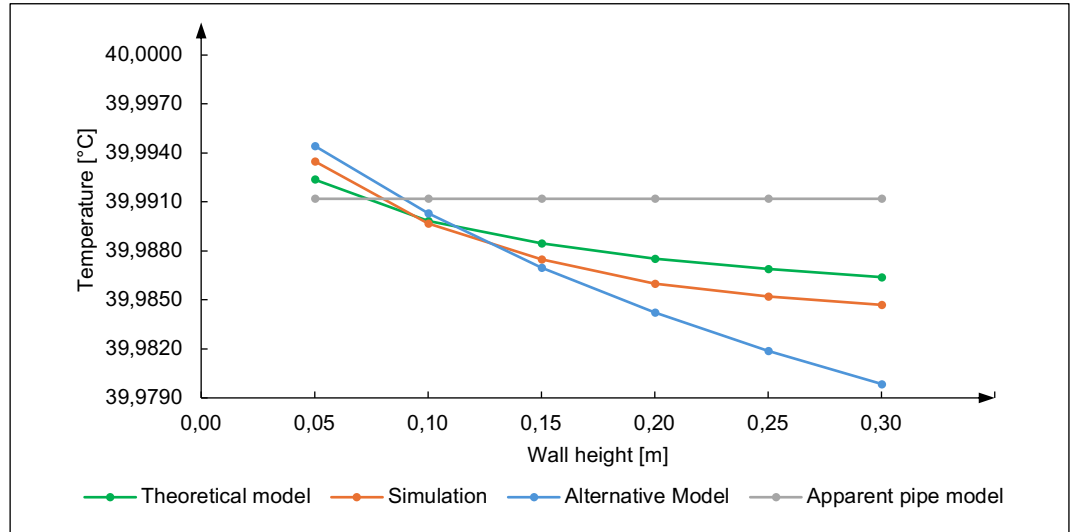


Figure 8 shows an intersection height of 0.0938 m that was obtained between the curves of the theoretical model and the simulation. It can be observed that the alternative model shows a temperature reduction close to that of these methods at the intersection height, indicating that, at this height, they exhibit similar values of thermal resistance of the mortar. Table 1 presents the intersection heights from the other graphs, as well as the mean calculated for both velocities and the height adopted for each diameter.

Table 1: Wall height for each pipe diameter.

Velocity (m s ⁻¹)	Intersection height (m)	Mean of intersection heights (m)	Adopted height (m)
DN20			
0,5	0,0938	0,0966	0,10
3,0	0,0994		
DN25			
0,5	0,0880	0,0845	0,10
3,0	0,0810		
DN32			
0,5	0,0763	0,0692	0,05
3,0	0,0622		

4.3 Second stage

A Figura 9 mostra a variação da temperatura a jusante em função da velocidade pelo modelo teórico e pela simulação para o diâmetro DN20.

Figure 9: Temperatura a jusante para o tubo DN20.

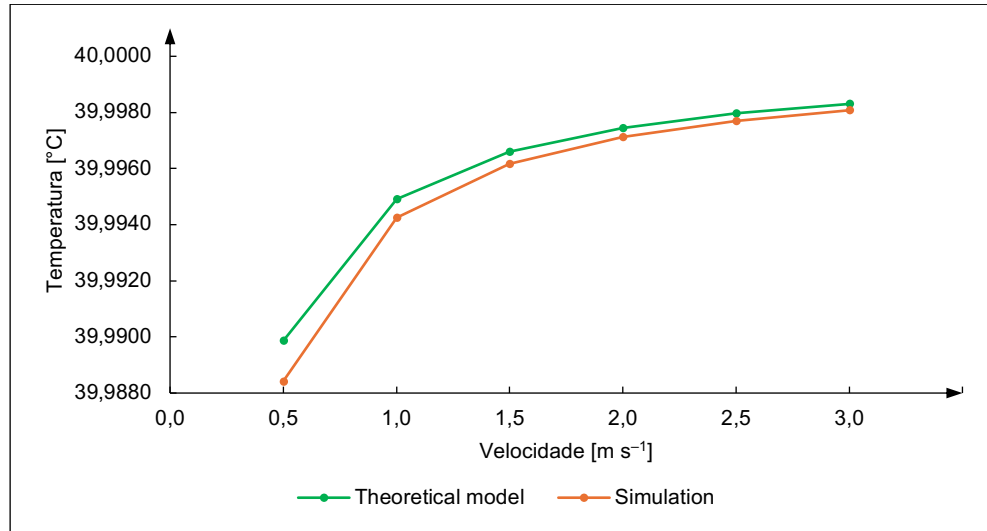


Table 2 presents the mean temperature reduction, the Shapiro-Wilk test statistic (*W*), and the *p*-value for each sample, all obtained in Jamovi. For all samples, the statistic value is higher than the critical value (0.792251), and the *p*-value is greater than the significance level of the test (5%), indicating normality in the samples and allowing the use of the paired samples *t*-test for the difference between the means of the two samples.

Table 2: Shapiro-Wilk test parameters.

	DN20		DN25		DN32	
	Theoretical model	Simulation	Theoretical model	Simulation	Theoretical model	Simulation
Mean (°C)	0,004149	0,004712	0,002735	0,003118	0,001289	0,001269
<i>W</i>	0,802359	0,799306	0,802278	0,801745	0,802072	0,803371
<i>p</i> -value	0,061712	0,057935	0,061607	0,060934	0,061347	0,063011

Table 3 presents the values of the mean differences, standard deviation, standardized *t*-test statistic, and *p*-value for each pipe diameter. For a confidence level of 95% and 5 degrees of freedom, the critical value for rejecting the null hypothesis is 2.571 (Larson, 2023). Therefore, the values of the standardized test statistic for acceptance of the null hypothesis must fall between -2.571 and 2.571.

Table 3: Test-*t* parameters.

DN (mm)	Mean of the Differences Between Paired Data Values (°C)	Standard deviation of the differences (°C)	Standardized test statistic	<i>p</i> -value
20	0,000563	0,000458	2,7516	0,02961
25	0,000383	0,000282	3,0391	0,02080
32	0,000020	0,000025	-1,7975	0,10603

The results of the test statistic and the *p*-value indicate that for DN20 and DN25 pipes, the null hypothesis should be rejected, while for the DN32 pipe, it can be accepted. This shows that, at a 95% confidence level, it can be stated that there is a significant difference

between the temperature reductions predicted by the theoretical model and those obtained from simulations for DN20 and DN25 pipes. For the DN32 pipe, it is concluded that there is no significant difference between the results.

These differences may have been caused by the varying characteristics of the theoretical model and the simulations. In the theoretical model, it is important to consider the influence of empirical correlations, the conduction shape factor, and the equations governing radiation. Although the correlations were chosen to meet the problem's conditions, it should be noted that they were developed experimentally, and according to Incropera *et al.* (2008), using certain correlations for convection can result in errors of up to 25%.

Regarding the shape factor, the pipe was considered to be centered in the masonry section to select the shape factor presented in the literature. However, this position differs from the usual arrangement of the pipe near the wall face, which was simulated in Fluent. The simplification of the radiation modeling, which considers the energy exchange between the wall and a neighboring surface, also significantly influences the results, as the heat transfer coefficient by radiation is strongly dependent on the temperature of the wall surface.

In the simulations, the results are affected by the quality of the mesh, which, in the version of Fluent used in this work, has a limitation on the number of generated elements. Similar to empirical correlations, the $k - \varepsilon$ turbulence model is semi-empirical, and using it may lead to discrepancies compared to exact results. Furthermore, the need to provide the program with an estimate of the natural convection coefficient indicates a flaw in the simulation, as the value supplied facilitates the approximation of the solution to the theoretical model's result.

Although the results were significantly different for DN20 and DN25 pipes, the percentage difference between the reductions was analyzed to verify if this value remains constant as the water flow velocity varies. The results are presented in Table 4.

Table 4: Percentage differences between the temperature reductions.

Velocity (m s ⁻¹)	Difference between the reductions (%)	
	DN20	DN25
0,5	14,19	13,70
1,0	13,19	13,85
1,5	12,86	13,99
2,0	13,27	14,35
2,5	13,21	14,66
3,0	13,26	14,95

For the DN20 pipe, a mean difference of 13.33% with a standard deviation of 0.45% was obtained. For the DN25 pipe, the results were a mean of 14.25% and a standard deviation of 0.49%. The values found for the standard deviation are small relative to the mean, leading to the conclusion that the difference between the theoretical model and the simulation remains approximately constant for the considered velocities.

Based on these analyses, it is considered that the theoretical model provides results close to those obtained from the simulations, and thus the formulations can serve as a viable option for estimating thermal loss in PN 25 PPR pipes embedded in masonry. However, the limitations in the simulations highlight the need for conducting experiments to achieve a more thorough comparison and complete validation of the model.

4.4 Temperature Loss in a Hot Water System of a Single-Family Residence

Table 5 shows the temperatures at the points of use for each appliance in the residence, as well as the temperature reductions compared to the water temperature at the heater output, the energy losses in the pipeline, the energy used for heating, and the percentage of energy loss.

Table 5: Temperature at the points of use and energy losses.

Point of use	Temperature (°C)	Reduction (°C)	Heat loss (W)	Heating cost (W)	Percentage of energy loss (%)
Sink	39,9289	0,0711	36,84	10367,21	0,36
Lavatório do lavabo	39,5189	0,4811	149,63	6220,32	2,41
Lavatório do banheiro	39,5474	0,4526	140,79	6220,32	2,26
Chuveiro	39,5573	0,4427	183,59	8293,76	2,21

Based on these results, it can be concluded that the energy loss was significantly greater when using the lavatories and the shower compared to using the sink. This is due to the distance between the heater and the sink, which is much shorter than the distance from the heater to the other points. Another factor contributing to the lower thermal loss for the sink is the high flow rate and velocity of the water flow, which results in a lower heat transfer rate compared to the other situations.

5 Conclusion

It is important to analyze thermal loss in hot water plumbing systems to understand energy expenditures and how materials and equipment perform. This study assessed the temperature reduction in PPR pipes embedded in masonry using a theoretical model. Unlike other methods of estimating thermal loss, this model considered all heat transfer modes in a real system and the pipe configuration embedded in masonry, a common situation in hot water systems for single-family homes. The model application in the residential project provided relevant information, such as the temperature at the points of use and the percentage loss of energy.

In the model analysis, it was observed that the temperature loss increased considerably with the wall height used in the calculation. Conversely, the loss decreases as the pipe diameter or flow velocity increases. CFD simulations were conducted to determine the appropriate wall height and to compare and evaluate the theoretical model. These simulations have the advantage of reducing the number of experiments, saving time and money. However, limitations in mesh quality and the need to input an estimated convection coefficient require conducting experiments for a more comprehensive analysis of height and complete validation of the model.

The statistical analysis, with a 95% confidence level, revealed that the mean temperature reductions from the theoretical model and simulations were significantly different for DN20 ($t = 2.7516$ and $p\text{-value} = 0.02961$) and DN25 ($t = 3.0391$ and $p\text{-value} = 0.02080$) pipes. However, the differences remained approximately constant as the flow velocity varied, with a mean difference of 13.33% and a standard deviation of 0.45% for the DN20 pipe, and a mean difference of 14.25% and a standard deviation of 0.49% for the DN25 pipe. For the DN32 diameter, no significant difference was found ($t = -1.7975$ and $p\text{-value} = 0.10603$). Given the conditions and limitations of both methods, it is considered that the two approaches yield similar results. Thus, it can be concluded that the methodology used in the model is promising and may serve as an option for estimating thermal loss in pipes.

For future work, it is recommended to conduct an experimental study to determine the temperature reduction in pipes embedded in masonry while varying the water flow velocity. Testing more advanced empirical correlations is suggested to reduce potential errors in calculations. Additionally, simulations using other turbulence models, such as $k - \omega$, should be conducted. This article focused solely on PPR pipes; however, the model has great potential for application with other materials, such as CPVC and PEX, due to their similar geometry to that of PPR pipes.

References

- AMANCO. **Manual técnico:** Linha amanco PPR. Joinville: [s.n.], 2010. Disponível em: http://assets.production.amanco.com.br.s3.amazonaws.com/uploads/gallery_asset/file/37/baixa_amco_atualizacao_manual_tecnico_amanco_PPR_2010_v11.pdf. Acesso em: 02 out. 2022.
- ANSYS INC. **ANSYS Fluent User's Guide.** Canonsburg: [s.n.], 2023. 5050 p.
- ANSYS INC. **Ansys Student - Free Software Download.** [s.n.], 2023. Disponível em: <https://www.ansys.com/academic/students/ansys-student>. Acesso em: 17 ago. 2023.
- ASSOCIAÇÃO BRASILEIRA DE NORMAS TÉCNICAS. **NBR 15813-1:** Sistemas de tubulações plásticas para instalações prediais de água quente e fria Parte 1: Tubos de polipropileno copolímero random PP-R e PP-RCT – requisitos. Rio de Janeiro, 2018. 41 p.
- ASSOCIAÇÃO BRASILEIRA DE NORMAS TÉCNICAS. **NBR 5626:** Instalação predial de água fria. Rio de Janeiro, 1998. 41 p.
- ASSOCIAÇÃO BRASILEIRA DE NORMAS TÉCNICAS. **NBR 5626:** Sistemas prediais de água fria e água quente – projeto, execução, operação e manutenção. Rio de Janeiro, 2020. 63 p.
- BENEDICTO, S. M. de O. **Desempenho de sistema predial de água quente.** 200 f. Dissertação (Mestrado em Construção Civil) – Universidade Federal de São Carlos, São Carlos, 2009.
- BORGES, T. P. de F. **Síntese Otimizada de Sistemas de Aquecimento Solar de Água.** 139 f. Tese (Doutorado em Engenharia Mecânica) – Faculdade de Engenharia Mecânica, Universidade Estadual de Campinas, Campinas, 2000.
- BORGNAKKE, C.; SONNTAG, R. E. **Fundamentos da termodinâmica.** 8. ed. São Paulo: Blücher, 2018. 730 p.
- BOTELHO, M. H. C.; RIBEIRO JUNIOR, G. de A. **Instalações hidráulicas prediais utilizando tubos plásticos.** 4. ed. São Paulo: Blücher, 2014. 416 p.
- BRUNETTI, F. **Mecânica dos fluidos.** 2. ed. São Paulo: Pearson Prentice Hall, 2008. 430 p.
- CARDOSO, R. M.; DAMO, R. A. Z.; MATTER, R. M. **Estudo da perda de calor nas tubulações de água quente em parede de alvenaria.** 94 f. Trabalho de Conclusão de Curso (Graduação em Engenharia Mecânica) – Centro Universitário Positivo, Curitiba, 2007.
- CHAGURI JUNIOR, J. J. **Sistemas prediais de aquecimento de água a gás:** parâmetros de dimensionamento e gerenciamento. 104 f. Dissertação (Mestrado em Energia) – Universidade de São Paulo, São Paulo, 2009.
- INCROPERA, F. P. *et al.* **Fundamentos de transferência de calor e de massa.** 6. ed. Rio de Janeiro: LTC, 2008. 643 p.
- FREI, F. **Introdução à inferência estatística:** aplicações em saúde e biologia. 1. ed. Rio de Janeiro: Interciência, 2018. 564 p.

- LARSON, R. **Estatística aplicada: Retratando o mundo.** 8. ed. São Paulo: Pearson, 2023. 581 p.
- MORAN, M. J. *et al.* **Introdução à engenharia de sistemas térmicos: termodinâmica, mecânica dos fluidos e transferência de calor.** 1. ed. Rio de Janeiro: LTC, 2005. 604 p.
- NATIONAL INSTITUTE OF STANDARDS AND TECHNOLOGY. **mini-REFPROP - Version 10.0.** 2020. Disponível em: <https://trc.nist.gov/refprop/MINIREF/MINIREF.HTM>. Acesso em: 05 ago. 2022.
- PORTO, R. M. **Hidráulica básica.** 4. ed. São Carlos: EESC-USP, 2006. 540 p.
- ŞAHIN, M. D.; AYBEK, E. C. Jamovi: an easy to use statistical software for the social scientists. **International Journal of Assessment Tools in Education**, v. 6, n. 4, p. 670–692, 2019.
- SILVA, C. V. da. **Introdução ao Ansys CFX.** Erechim: Universidade Regional Integrada do Alto Uruguai e das Missões, 2019. 44 p.
- TIGRE. **PPR: Termofusão: Catálogo técnico.** Joinville: [s.n.], 2012. Disponível em: <https://www.tigre.com.br/themes/tigre2016/downloads/catalogos-tecnicos/ctppr-termofusao.pdf>. Acesso em: 01 out. 2022.
- UEHARA, T.; FERREIRA, A. T. Decaimento de temperatura em tubos de PPR PN 25 embutidos em alvenaria. **Encontro de Iniciação Científica e Pós-Graduação IFSP – Campus São Paulo**, v. 7, 2022.
- UEHARA, T.; FERREIRA, A. T. Decaimento de temperatura em tubos de PPR PN 25 embutidos em alvenaria. **Congresso de Inovação, Ciência e Tecnologia do IFSP**, v. 13, 2022.
- UEHARA, T.; NASCIMENTO, C. H. B.; FERREIRA, A. T. Decaimento de temperatura em tubulações de PPR PN 25 para condução de água quente. **Revista Técnico-Científica de Engenharia Civil Unesc**, v. 7, n. 1, 2022.
- VERSTEEG, H. K.; MALALASEKERA, W. **An Introduction to Computational Fluid Dynamics: The finite volume method.** 2. ed. Inglaterra: Pearson Education, 2007. 503 p.
- YU, L. *et al.* Polypropylene random copolymer in pipe application: Performance improvement with controlled molecular weight distribution. **Thermochimica Acta**, Elsevier, v. 578, p. 43–52, 2014.
- YWASHIMA, L. A.; ILHA, M. S. de O.; FERREIRA, A. T. Tempo de recuperação da temperatura no sistema de recirculação de água quente. **Simpósio Brasileiro de Recursos Hídricos**, v. 22, 2017.